SHORT COMMUNICATIONS

A novel endorectal RF coil for high resolution MRI and spectroscopy of the prostate*

ZHANG Hongjie[1,2], SONG Xiaoyu[1], WANG Xiaoying[3], XU Pingfang[1] and BAO Shanglian[1]**

(1. Beijing Key Laboratory of Medical Physics & Engineering, Peking University, Beijing 100871, China; 2. Navy General Hospital, Beijing 100037, China; 3. Peking University First Hospital, Beijing 100034, China)

Received August 29, 2004; revised November 15, 2004

Abstract The diagnosis of prostate diseases by magnetic resonance imaging (MRI) *in vivo* is sometimes difficult for the lower signal to noise ratio (SNR). To increase the SNR of the prostate image, we designed a RF coil that can be inserted into rectum and was named endorectal coil. The properties of RF coil were evaluated using a network analyzer. Moreover the images and spectroscopy of a special phantom were acquired and the results were compared to those of the commercial TORSO coil (G.E. Medical Systems, USA). Our coil gave a significantly higher SNR at the region of interest (ROI). The achieved high local SNR and resulting high spatial resolution would add more anatomic and biochemical information to the diagnosis of prostate diseases.

Keywords: MRI, RF coil, endorectal coil.

MRI is a non-invasive powerful imaging tool and has been used in the diagnosis of various prostate diseases. The excellent soft-tissue contrast provided by MRI allows improved visualization of the prostate anatomy, surrounding critical structures (such as the neurovascular bundles and periurethral zone), and the extent of tumor spread. This improved contrast resolution presents a distinct advantage over other prostate imaging modalities such as transrectal ultrasound and computer tomography (CT). Consequently MRI has been used in the management of prostate cancer as a tool for preoperative evaluation[1—3], cancer staging[4], and image guidance of prostate interventions[3—5]. However, due to a lower SNR, current prostate MRI techniques still cannot provide sufficient image resolution to clearly visualize all features of interest. Because the RF coil is the first element of the receiver chain, it determines the obtainable SNR and thus is critical to the quality of the image obtained[5].

In order to improve the SNR, we developed a novel intracavitary receiver coil for prostate imaging. In the study, we used the body coil as the RF transmit coil, and our coil acted as the receiver coil. Then the MR images and MR spectroscopy of a special phantom were acquired. The results showed that our design offered a dramatic improvement of the SNR.

1 Materials and methods

1.1 Coil design

In order to optimize the coil, we considered the parameters affecting the SNR. Following a 90° pulse, the SNR of MRI signal is given by[6]

$$\Psi_{\mathrm{SNR}} = KM_0\left[\left(\frac{\omega_0 L}{R}\right)\frac{\eta\mu_0 V_S}{8kT\Delta f}\right]^{\frac{1}{2}} = KM_0\eta\left(\frac{\mu_0 Q\omega_0 V_c}{8kT\Delta f}\right)^{\frac{1}{2}},$$

where η, the "filling factor", is a measure of the fraction of the coil volume occupied by the sample, Q is the quality factor of the receive coil, K a numerical factor (≈ 1), M_0 the nuclear magnetization which is proportional to the field strength, μ_0 the permeability of free space, ω_0 the Larmor frequency, V_c the volume of the coil, K the Boltzmann constant, T the temperature during data acquisition, and Δf the bandwidth of the receiver in Hertz. It can be seen that among these parameters, the filling factor η and quality factor Q are leading ones concerned with the coil, hence we regarded them as the main parameters

* Supported by National Natural Science Foundation of China (Grant No. 10175004)

** To whom correspondence should be addressed. E-mail: bao@pku.edu.cn

for optimizing.

The coil was designed in a loop LC serial resonance circuit mode. Schematic diagram is shown in Fig. 1. It is composed of three units: a single loop coil, a coaxial cable, and a tuning/matching unit. The single-loop coil, which is the key part of the endorectal coil, together with the tuning capacitor C_t and the distributed inductance of the coaxial cable builds the resonant circuit. The nonmagnetic small-diameter 50 Ohm coaxial cable is used to convey the signal of single-loop coil to the tuning and matching unit. The matching circuit is achieved by using a standard impedance network consisting of nonmagnetic chip capacitors C_m and distributed inductance, which transform the coil impedance to 50 Ohm. The decoupling circuit is composed of a PIN diode and a tank circuit, which is constituted of C_m and a special coaxial cable. The function of the decoupling circuit is as follows: During RF transmission phase, MRI triggers a DC bias voltage that switches on the PIN diode, then, the LC tank circuit acts and presents very high impedance to the coil. Thus the coil is decoupled from the body coil to avoid the interfering from powerful RF source.

We increased the Q value by using nonmagnetic "case A-size" high-quality ceramic chip capacitor (ATC, USA) as the C_t and C_m. To ensure the coil was adjustable and had more homogeneous B_1 field, a thin flexible copper-silver wire loop was used as the distributed inductance. Furthermore, in order to ensure the coil easily pass through the rectum and fit into the prostate tightly, we ensheathed the coil circuit into a well-designed mechanical device[1)], which can be delivered into the anus smoothly. When the coil reached the nearest position to prostate, it expanded to be an ellipse shape, fitting into the prostate tightly and hence got a higher filling factor η, which helps to improve the SNR of images.

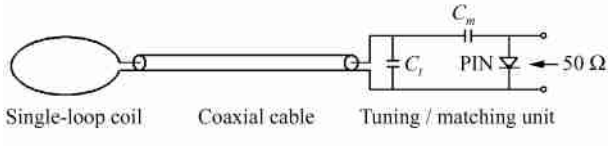

Fig. 1. Schematic diagram of our novel design. The tuning capacitor C_t together with the inductance of coil and coaxial cable builds a resonant circuit. The matching capacitor C_m matches the impedance of the circuit to 50 Ω. The PIN diode acts as a detuning device.

1.2 Test of the coil

We used an advanced network analyzer (HP 8712C, Palo Alto, CA) to test the coil. In order to simulate the loading conditions used in clinical situation[9], we constructed a phantom made of a polyethylene container (15 cm × 20 cm × 25 cm) and filled with 0.9% NaCl solution. After the coil was fixed in the phantom, we applied the analyzer's reflection measurement function, tuned the resonant frequency to 63.86 MHz (the Larmar frequency of 1.5T MR scanner, Fig. 2(a)), and then traced the smith chart. The coil impedance was adjusted to 50 Ohm (Fig. 2(b)) to match the impedance of MRI preamplifier.

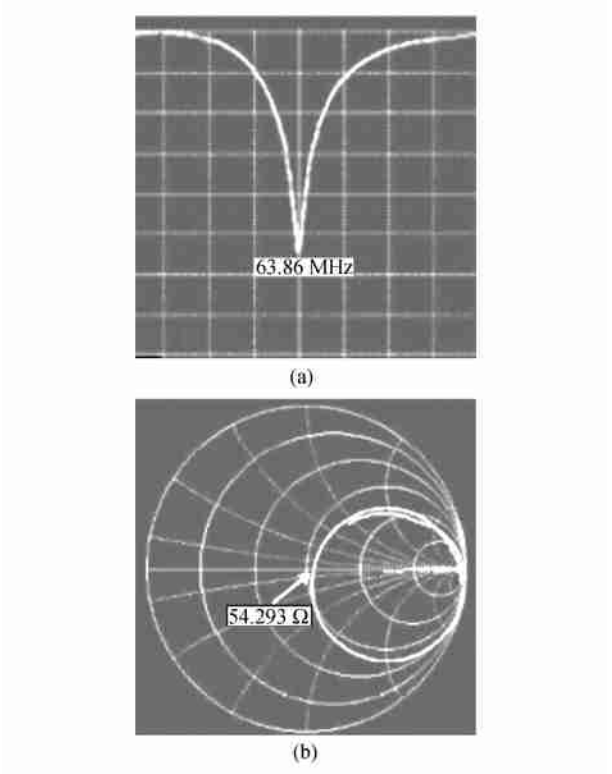

Fig. 2. Illustration of the coil properties of both tuning and matching obtained with the aid of a network analyzer. (a) Estimation of reflection (resonance frequency), (b) the Smith chart of nearly 50 ohm-matching of the endorectal design coil.

The quality factor Q was measured as the ratio of center frequency to bandwidth under both loaded and unloaded conditions. Bandwidth was estimated as the full width at half maximum of the resonance peak[10].

1) Zhang H. J. et al. China Patent (Application No. 2004100298171, 2004-10-02)

1.3 Magnetic resonance imaging and spectroscopy

In order to confirm our design and test it in MRI scanner, another special phantom was applied to the study. The phantom consisted of six cubes with a size of 6 cm× 10 cm× 12 cm each, a sphere in diameter of 10 cm and a Teflon tube which simulated rectum. All six cubes were filled with solution of Na_2SO_4. The sphere that represents the prostate was filled with the solution of 600 mL containing approximate physiological concentrations of the major prostate metabolites (Choline 4 mmol/L, creatine 10 mmol/L, Citrate 33 mmol/L, and lactate 12 mmol/L). All of these parts were arranged to simulate the real situation for prostate and its surrounding environment. Fig. 3 shows the images of the special phantom with parameters of: FSE, TR= 1000, TE= 90, FOV= 24× 24, 5 mm thk/1.5 mm SP, 256× 192, 1NEX.

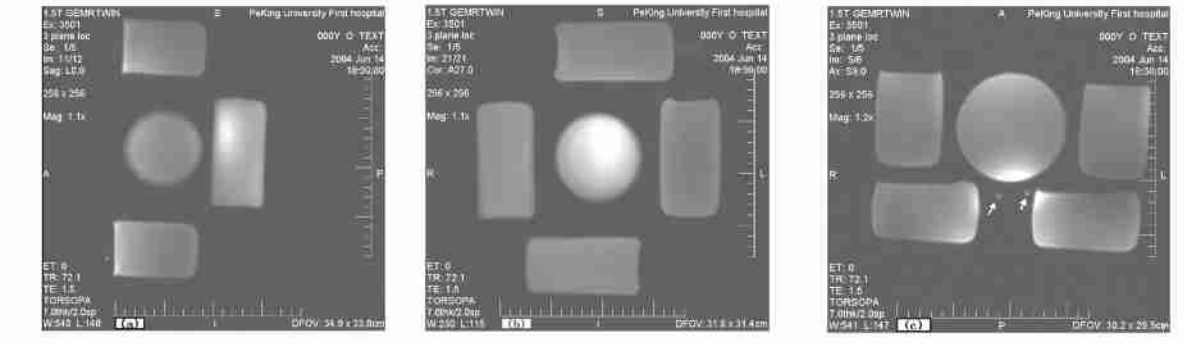

Fig. 3. Phantom images. (a)—(c) are sagittal, coronary and axial localizer images respectively. The two arrows in (c) indicate the cross section of the endorectal coil.

All studies were performed on a General Electric Signa 1.5 Tesla MR Scanner with advanced gradients (40 mT/m, 150 mT/m/ms). This system is augmented with a SGI Workstation (Silicon Graphic Inc., USA) for real-time data acquisition, data transfer, image reconstruction, and interactive control. RF excitation was achieved by using the whole body birdcage coil, and the MR signal was received using our endorectal coil and the commercial TORSO coil (G. E. Medical Systems, USA). The images were acquired using the sequence of FSE with the parameters of TR/TE= 3000/85 ms, ETL= 17, FOV= 13 mm× 13 mm, NEX= 1, and 3 mm slice thickness. The spectroscopic images were acquired with the point-resolved-spectroscopy (PRESS) double spin echo technique[2,3], the parameters were set to TR= 1 s, TE= 130 ms, FOV= 50 mm× 50 mm× 50 mm, 8× 8× 8 matrix, 9 min scan time, and the resolution of MRSI was 1.0 cm^3. A square volume (Fig. 4(a)) was selected as the ROI for the spectroscopic measurement. Prior to the spectroscopic imaging, the water signal from the volume was shimmed automatically by the commercial software of the scanner. The suppression of water and lipid was performed using the BASING technique[8—11]. As the images and spectral data were transferred to the SGI Workstation, they were processed with the corrections of receiving sensitivity profile. In addition, the spectral data were further processed with 2 Hz Lorentzian

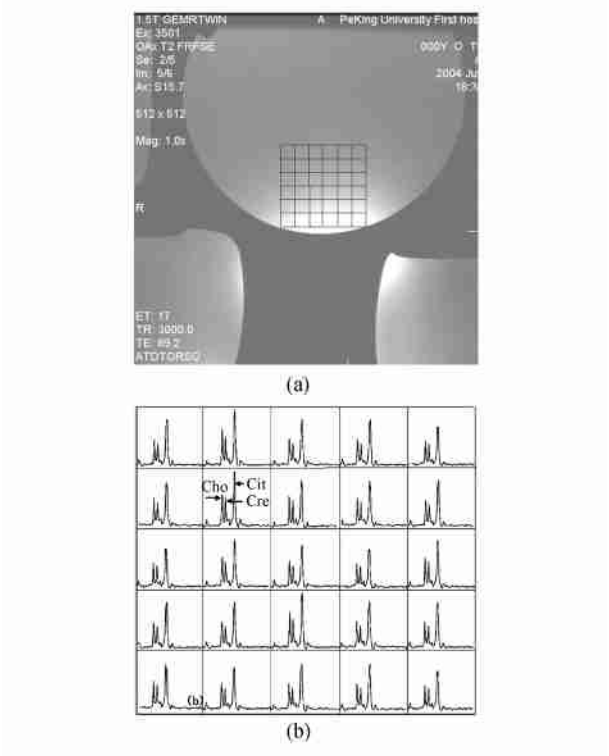

Fig. 4. The MRSI voxels corresponding to the grid overlaid on the image are shown in (a), and the 5× 5 grid MRSI data shown in (b). MRSI acquisition parameters: PRESS voxel selection with dual-BASING water and lipid suppression, TR 1 s, TE 130 ms, FOV 50 mm× 50 mm× 50 mm, 8 mm× 8 mm× 8 mm matrix, 9 min scan time. MRSI resolution is 1 cm^3.

apodization in the time domain followed by three-dimensional Fourier transform and automated frequency, phase and baseline correction using a combined software. The peak areas of Cho, Cr, and Cit were calculated by numerical integration over the spectral ranges corresponding to each metabolite, the 5×5 grid MRSI data is shown in (Fig. 4(b)).

2 Results and discussions

The quality factor Q was calculated as the ratio of center frequency to bandwidth. The bandwidth was estimated as the full width at half maximum of the resonance peak. According to the results from the network analyzer, the unloaded and loaded quality factors Q for our new designed rectum RF coil were 277 and 78 respectively.

The SNR of the TORSO coil (G. E. Medical Systems, USA) was compared with our endorectal coil. A 4.1 cm^2 ROI (see Fig. 5) was used to measure the mean signal intensity and standard deviation from the images. The SNR of each image was calculated with the method of dividing the mean signal intensity in the selected ROI by the noise from background area. The noise from background area was calculated by multiplying the measured standard deviation in the background by 1.4 to account for the rectified signal due to the magnitude operation. Fig. 5 (a) is a phantom image acquired using the TORSO coil, from which we can see that the mean signal intensity is 153.4 and standard deviation is 1.5; (b) image acquired using the endorectal coil, the mean signal intensity and standard deviation are 500.5 and 1.3 respectively. Using the above method, the SNR of the TORSO coil image was found to be 73 and that of the endorectal was 275. Results showed that the SNR of the endorectal coil was higher than the TORSO coils' in all ROI evaluated at least 3.7 times.

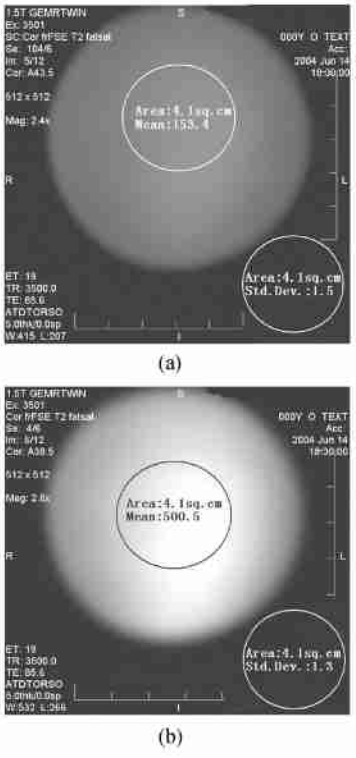

Fig. 5. T2-weighted axial images of the prostate phantom (FOV 13×13 cm, slice thickness 3 mm). (a) Acquired using the TORSO coil, (b) using the endorectal coil. A 4.1 cm^2 ROI was used to measure the mean signal intensity on the phantom images and standard deviation on the background area, that of the TORSO coil was 153 and 1.5; that of the endorectal coil was 500.5 and 1.3 respectively.

From Fig. 6, we could see that the region of high SNR of the endorectal coil is approximately a volume of 3.6 cm×7.3 cm×8.7 cm, which is sufficient to cover the full area of the prostates in whatever normal or pathological state (3 cm×4 cm×5 cm)[3]. The results also showed that the coil could be used for high SNR spectroscopy of the metabolic peaks relevant to prostate metabolites, which are choline, creatine, and citrate at the shifted positions of 3.2, 3.0 and 2.6 parts per million (ppm) respec-

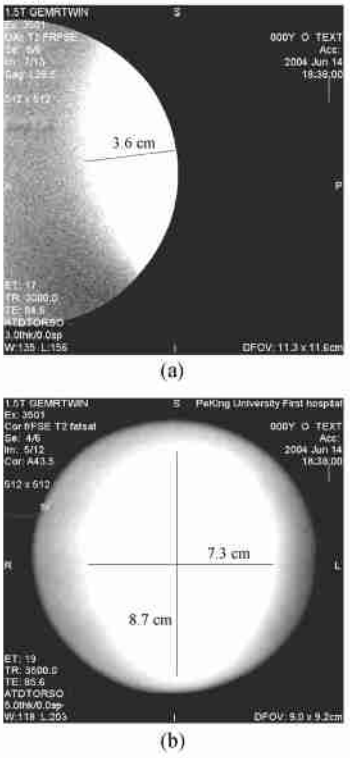

Fig. 6. The prostate phantom sagittal (a) and axial image (b) acquired with our endorectal coil. The volume of high SNR is about 3.6 cm×7.3 cm×8.7 cm.

tively and shown in Fig.7.

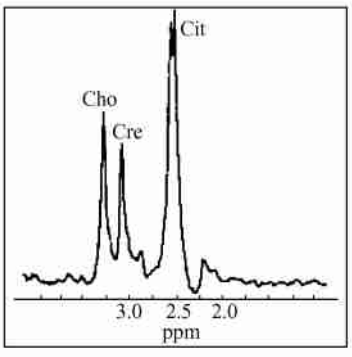

Fig. 7. MR spectral trace obtained from MRSI. The metabolic peaks occurring at downward frequency shift relative to water of approximately 3.2, 3.0 and 2.6 ppm respectively.

Recent studies have demonstrated that MRSI of the prostate can effectively distinguish the regions of cancer from normal tissues, even grade the process of the malignant of prostate[1,5,6,11—13].

3 Conclusion

We have developed a shape-adjustable coil for the prostate diagnosis. The small diameter and the expandable design enables it to be easily used in clinical practice. The phantom imaging study demonstrated that the size of the coil is sufficient to cover the full area of the prostate with higher SNR. It has a high performance in both space resolution of the images and high SNR spectra of prostate metabolites.

Acknowledgement The authors are grateful to Prof. Zu Donglin (Peking University) for his enthusiastic help in the building of the coil, to Li Sha (The Peking University First Hospital) for his comments and encouragement, and to Dr. Sun Fei of GE Medical Systems for his continuous support.

References

1 Coakley V. F., Aliya Q., John K. et al. Magnetic resonance imaging and spectroscopic imaging of prostate cancer. Journal of Urology, 2003, 170: 69—76.
2 Jarle R. and Svein H. Magnetic resonance imaging of the prostate. Current Opinion in Urology, 2001, 11(2): 181—188.
3 Myers R. P., Cahill D. R., Devine R. M. et al. Anatomy of radical prostatectomy as defined by magnetic resonance imaging. Journal of Urology, 1998, 159(6): 2148—2151.
4 Sonnad S. S., Langlotz C. P., Schwartz J. S. et al. Accuracy of MR imaging for staging prostate cancer: a meta-analysis to examine the effect of technologic change. Acad. Radio., 2001, 8: 149—157.
5 Harald H. Q., Mark E. L., Gesine G. et al. Single-loop coil concepts for intravascular magnetic resonance imaging. Magnetic Resonance in Medicine, 1999, 41: 751—758.
6 Hoult D. I. and Richards R. E. The signal-to-noise ratio of the nuclear magnetic resonance experiment. J. Magn. Res., 1976, 24: 71—85.
7 Song X. Y., Wang W. D., Zhang B. D. et al. Digitalization decoupling method and its application to the phase array in MRI. Progress in Natural Science, 2003, 12: 683—689.
8 Engelbrecht M. R. Local staging of prostate cancer using magnetic resonance imaging: a meta-analysis. Eur. Radio., 2002, 12: 2294—2298.
9 Kurhanewicz J. Three-dimensional magnetic resonance spectroscopic imaging of brain and prostate cancer. Neoplasia, 2002, 2: 166—172.
10 Schricker A. A., Pauly J. M., Kurhanewicz J. et al. Dual band spectral-spatial RF pulses for prostate MR spectroscopic imaging. Magnetic Resonance in Medicine, 2001, 46: 1079—1087.
11 Star L. J., Lee R., Baertlein B. A. et al. Improved water and lipid suppression for 3D PRESS CSI using RF band selective inversion with gradient dephasing (BASING). Magnetic Resonance in Medicine, 1997, 38: 311—319.
12 Gabriel H. and Joseph P. M. MR imaging of prostate disorders. Radiographics, 1994, 14: 763—769.
13 Atalar E., Bottomley P. A., Ocali O. et al. High resolution intravascular MRI and MRS by using a catheter receiver coil. Magnetic Resonance in Medicine, 1996, 36: 596—605.